

Bifunctional decamethylcyclohexasilanes $X_2Si_6Me_{10}$ ($X = Cl, H,$ or OH): molecular and crystal structures and mesomorphic properties

D. Yu. Larkin,^a A. A. Korlyukov,^{a*} E. V. Matukhina,^b M. I. Buzin,^a
N. A. Chernyavskaya,^a M. Yu. Antipin,^a and A. I. Chernyavskii^a

^aA. N. Nesmeyanov Institute of Organoelement Compounds, Russian Academy of Sciences,
28 ul. Vavilova, 119991 Moscow, Russian Federation.

Fax: +7 (095) 135 5085. E-mail: alex@xrlab.ineos.ac.ru

^bMoscow State Pedagogical University,

1 ul. Malaya Pirogovskaya, 119882 Moscow, Russian Federation.

Fax: +7 (095) 245 0310. E-mail: lmatukh@mail.ru

Isomer separation of mixtures, which were prepared by chlorination followed by transformations of dodecamethylcyclohexasilane $(Me_2Si)_6$ into bifunctional decamethylcyclohexasilanes $X_2Si_6Me_{10}$ ($X = Cl, H,$ or OH), was carried out. As a result, mixtures of the corresponding 1,3- and 1,4-derivatives were separated to obtain structural isomers, and stereoisomers, *viz.*, *cis*- and *trans*-1,4-dihydrocyclohexasilanes, were isolated in individual form. The molecular and crystal structures of the resulting bifunctional decamethylcyclohexanes $X_2Si_6Me_{10}$ ($X = H$ or OH) and decamethyl-7-oxahexasilanorbornane were established by X-ray diffraction analysis. Bifunctional cyclohexasilanes form a mesophase as a plastic crystal. The temperature range of its existence was determined.

Key words: bifunctional decamethylcyclohexasilanes; molecular and crystal structure; mesomorphic properties; X-ray diffraction analysis, DSC, polarization microscopy.

Bifunctional decamethylcyclohexasilanes $X_2Si_6Me_{10}$ ($X = Cl, H,$ or OH) are of great interest as starting compounds in the synthesis of different molecular-design polymers.^{1–3} Earlier,^{4–6} dichlorodecamethylcyclohexasilane $Cl_2Si_6Me_{10}$ has been prepared by the reaction of dodecamethylcyclohexasilane $(Me_2Si)_6$ (**1**) with $SbCl_5$ as a mixture of structural isomers, 1,3- and 1,4-dichlorodecamethylcyclohexasilanes (**2** and **3**, respectively) (Scheme 1). It has also been reported⁶ that the reaction of a mixture of dichlorocyclosilanes **2** and **3** with $LiAlH_4$ affords a mixture of 1,3- and 1,4-dihydrodecamethylcyclohexasilanes (**4** and **5**, respectively).

Separation of structural isomers is necessary for their use as starting compounds in the synthesis of polymers with required structure. Several procedures were developed^{4,6,7} for separation of isomers **2** and **3**. The simplest and most efficient procedure⁷ involves hydrolysis of a mixture of cyclohexasilanes **2** and **3** followed by separation of the reaction products by vacuum distillation. Cyclosilane **2** reacts with H_2O to form 1,3-dihydroxydecamethylcyclohexasilane (**6**), whereas cyclosilane **3** gives a mixture of 1,4-dihydroxydecamethylcyclohexasilane (**7**) and decamethyl-7-oxahexasilanorbornane (**8**), the latter being formed as a result of intramolecular condensation of cyclosilane **7**. Treatment of dihydroxycyclosilane **6** and a mixture of dihydroxycyclosilane **7** and

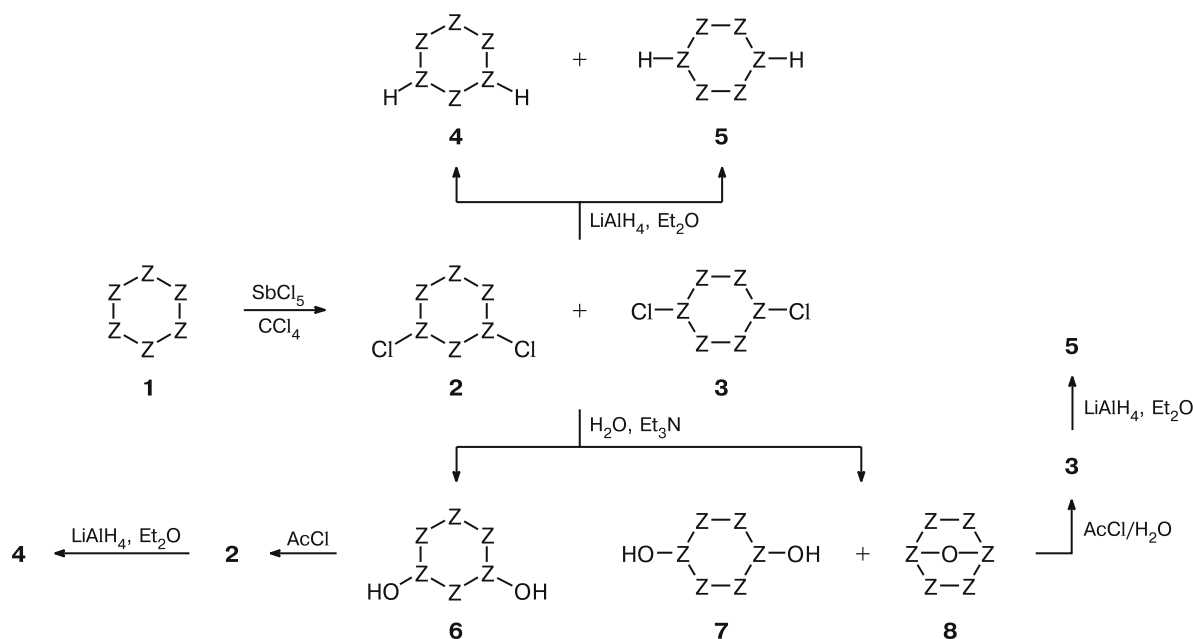
heterocycle **8** with acetyl chloride affords individual dichlorocyclosilanes **2** and **3**, respectively, in quantitative yield.⁷

X-ray diffraction study of hydrolysis products of 1,4-dichlorocyclosilane **3** showed⁷ that both 1,4-dihydroxycyclosilane **7** and heterocycle **8** are present in the unit cell in a ratio of 1 : 2. X-ray diffraction data for individual compounds **7** and **8** and 1,3-dihydroxycyclosilane **6** were lacking. More recently,⁸ we have studied the molecular and crystal structure of 1,3-dihydroxycyclosilane **6** by X-ray diffraction. The six-membered silane ring in compound **6** was demonstrated to adopt a chair conformation. The oxygen atoms are in a *cis*-diaxial orientation. In the crystal, molecules **6** are linked through medium-strength hydrogen bonds to form infinite chains running along the *a* axis.

Nowadays, only two permethylcyclosilanes, *viz.*, decamethylcyclopentasilane $(Me_2Si)_5$ and dodecamethylcyclohexasilane $(Me_2Si)_6$, which form a mesophase as a plastic crystal, are known.^{9–11} Data on the mesomorphic properties of disubstituted permethylcyclohexasilanes are lacking in the literature.

In the present study, we determined the molecular and crystal structures of bifunctional permethylcyclohexasilanes and examined the possibility of existence of these compounds in a mesomorphic state.

Scheme 1



Z = SiMe_n, n = 1, 2

Results and Discussion

Bifunctional cyclohexasilanes **2**–**7** were synthesized according to modified procedures^{6,7} (see Scheme 1). The reactions of a mixture of dichlorocyclohexasilanes **2** and **3** and individual cyclohexasilanes **2** and **3** with LiAlH₄ produced 1,3- and 1,4-dihydrocyclohexasilanes **4** and **5** as mixtures and individual compounds, respectively. *trans*-1,4-Dihydrocyclohexasilane (**5b**) was isolated from a mixture of structural isomers **4** and **5** by fractional crystallization. In the case of an individual structural isomer **5**, the *cis* (**5a**) and *trans* isomers (**5b**) were successfully separated and isolated (see the Experimental section). Unfortunately, we failed to separate the *cis* and *trans* isomers of 1,3-dihydrocyclohexasilane **4** by fractional crystallization.

X-ray diffraction study of bifunctional cyclohexasilanes **2–**7** and heterocycle **8**.** Single-crystal X-ray diffraction study of dichlorosubstituted cyclohexasilanes **2** and **3** revealed static disorder of all methyl groups and chlorine atoms, the Si–Si bond lengths being close to the standard value for these bonds. This result can be attributed to the fact that the crystals are composed of geometric isomers of cyclohexasilanes **2** and **3**, whose superposition is responsible for the observed disorder.

The presence of geometric isomers of dichlorocyclohexasilanes **2** and **3** in the crystals was confirmed by investigation of the crystalline products of their hydrolysis. Four crystalline phases were isolated. One of these phases (**A**), which has been described in our earlier study,⁸ contains

compound **6**. Two other phases (**B** and **C**) are cocrystals of compounds **7** and **8**. The fourth crystalline phase (**D**) contains only heterocycle **8**. The crystal structure of the phase **C** has been described earlier.⁷ However, we re-investigated this structure to perform its more thorough comparison. This allowed us to compare the crystal and molecular structures of the phases **B** and **C** in more detail.

The bicyclic moiety of compound **8** (Fig. 1) consists of two five-membered rings, which adopt an envelope conformation with the oxygen atom deviating from the basal plane, on the average, by 0.74 Å. The average angle between the Si(1)Si(2)Si(3)Si(4) and Si(1)Si(4)Si(5)Si(6) planes is 64.3°. Due to the presence of the bicyclic structure, steric hindrance in compound **8** is higher than that in other known cyclohexasilanes. This is evidenced by an average elongation of the Si–Si bonds by 0.02 Å compared to those in cyclohexasilanes **6** and **7** as well as by considerable variations in the Si–Si–Si angles (95–116°). In addition, the Si(1)–O(1) and Si(4)–O(1) bonds in the structure of compound **8** are somewhat shorter compared to those in the cocrystals **B** and **C**, which can be attributed to the involvement of the O(1) atom in a hydrogen bond with the hydroxy group of molecule **7**.

The six-membered ring of cyclohexane **7** (see Fig. 1) in the cocrystals **B** and **C** lies on a crystallographic inversion center and adopts a chair conformation with the Si(3') and Si(3A) atoms deviating from the plane formed by the other atoms by 1.019 and 1.055 Å in **B** and **C**, respectively. The hydroxy groups are in pseudoequatorial positions

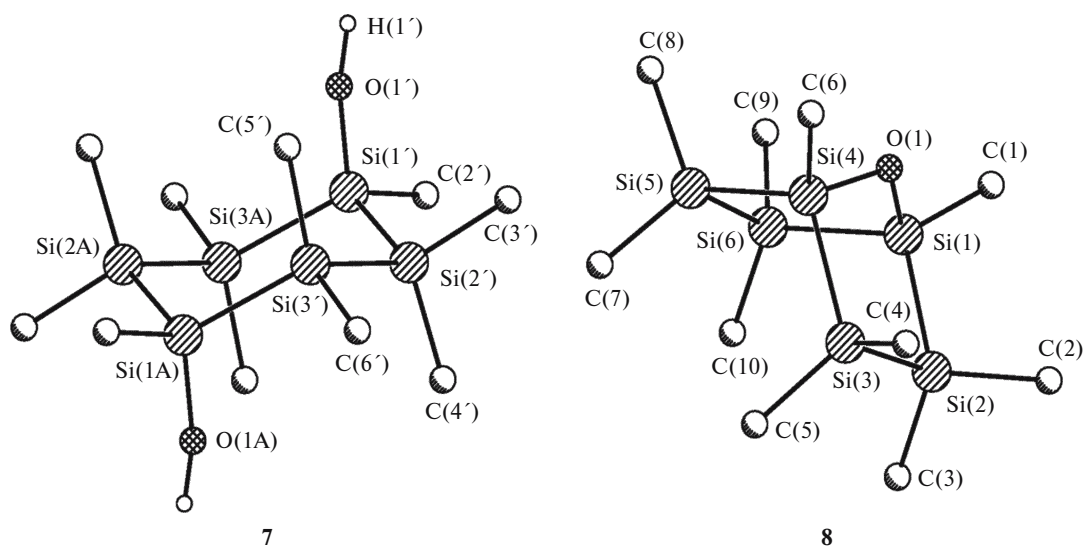


Fig. 1. Overall view of molecules **7** and **8** in the cocrystals **B** and **C**. The hydrogen atoms, except for H(1'), are omitted.

(the O(1')Si(1')Si(1A)O(1A) pseudotorsion angle is 180°). In the cocrystal **B**, the Si(1')—Si(2'), Si(2')—Si(3'), and Si(1')—Si(3A) bond lengths are virtually equal to each other (Table 1), whereas these bond lengths in the cocrystal **C** vary within 0.02 Å. This can be attributed to $n-\sigma^*$ interactions between the lone pairs (LP) of the oxygen atoms and the antibonding orbitals of the Si—Si bonds. Actually, the pseudotorsion angles between the LP of the oxygen atoms and the Si(1')—Si(3A) and Si(1')—Si(2') bonds in the cocrystal **C** are close to 180°. By contrast, the analogous angles in the cocrystal **B** are, on the average, 90°. The Si—C bond lengths are in the

range of 1.87–1.89 Å, whereas the Si—O bond lengths are 1.67–1.68 Å.

In the cocrystals **B** and **C**, molecules **7** and **8** are linked into O—H...O-bonded trimers. The hydroxy groups of the central cyclosilane molecule **7** form hydrogen bonds with the oxygen atoms of the terminal molecules of heterocycle **8** (Fig. 2). It should be noted that the O...O distance in the cocrystal **C** is ~0.3 Å longer than that in the cocrystal **B**. The crystalline phase **B** has been previously unknown. Hence, it was interesting to quantitatively characterize the cocrystals **B** and **C**, which requires quantum-chemical calculations for their crystal packings.

Table 1. Selected bond lengths and bond angles in the crystals **B**, **C**, **D**, and **5b** and isolated molecules **7** and **8**

Bonds (Å) and angles (deg)	Crystal				Isolated molecule (calculations)	
	Experiment/calculations		Experiment		7	8
	B	C	D	5b		
Si(1)—O(1)	1.686(2)/1.719	1.692(2)/1.723	1.683(2)			1.704
Si(4)—O(1)	1.692(2)/1.720	1.696(2)/1.721	1.681(2)			1.704
Si(1')—O(1')	1.672(4)/1.688	1.678(2)/1.684			1.702	
Si(1)—Si(2)	2.379(1)/2.395	2.375(1)/2.387	2.367(1)	2.337(1)		2.386
Si(1)—Si(6)	2.360(1)/2.382	2.345(1)/2.364	2.364(1)	2.339(1)		2.384
Si(2)—Si(3)	2.365(1)/2.379	2.354(1)/2.374	2.370(1)	2.339(1)		2.385
Si(3)—Si(4)	2.367(1)/2.372	2.364(1)/2.380	2.379(3)			2.385
Si(4)—Si(5)	2.358(1)/2.389	2.360(1)/2.376	2.365(1)			2.385
Si(5)—Si(6)	2.365(1)/2.377	2.354(1)/2.374	2.365(1)			2.385
Si(1')—Si(2')	2.351(1)/2.368	2.339(1)/2.367			2.377	
Si(1')—Si(3A)	2.355(2)/2.388	2.339(1)/2.378			2.375	
Si(2')—Si(3')	2.337(1)/2.350	2.338(1)/2.349			2.367	
Si—C	1.889/1.901	1.884/1.902	1.880	1.897	1.903	1.903
Si(1)—O(1)—Si(4)	116.6(1)/114.2	115.9(1)/114.7	116.6(1)			116.3
O(1')—Si(1')—Si(2')	102.9/103.6	110.05(9)/109.3			109.3	
O(1')—Si(1')—Si(3'A)	115.7/112.0	104.25(9)/104.3		108.89(7)	109.1	

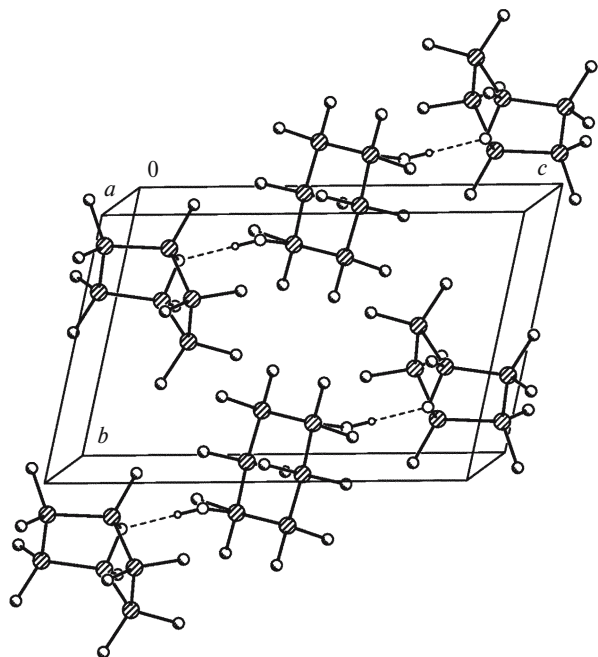


Fig. 2. O—H...O-Bonded trimers in the cocrystals **B** and **C**. The parameters of the O—H...O hydrogen bonds: O(1')...O(1), 3.138(4) Å; O(1)...H(1'), 2.16 Å; O(1')—H(1')...O(1), 169° (**B**); O(1')...O(1), 2.811(3) Å; O(1)...H(1'), 1.99 Å; O(1')—H(1')...O(1), 157° (**C**).

For this purpose, we carried out quantum-chemical calculations of isolated molecules **7** and **8** and the crystal packings of **B** and **C**. On the whole, the calculated geometric parameters of the molecules in the free state agree well with those in the crystals. The Si—Si and Si—O bond lengths are overestimated, on the average, by 0.03 and 0.02 Å, respectively (see Table 1). The Si(1)—O(1) and Si(4)—O(1) bond lengths are most noticeably overestimated, the differences between the calculated and experimental bond lengths being as large as 0.03 Å. The calculated lengths of the corresponding bonds in molecule **7** differ from the experimental values by at most 0.015 Å. Apparently, an overestimation of the Si—Si and Si—O bond lengths is a common drawback of calculations by the density functional theory. For example, quantum-chemical calculations for octamethyl-1,4-dioxo-2,3,5,6-tetrasilacyclohexane by the B3LYP/6-311G(d) method¹² substantially overestimated the Si—Si and Si—O bond lengths. The Si—C bond lengths were reproduced with higher accuracy (the average discrepancy was 0.01 Å).

In the cocrystal **B**, the calculated O(1)...O(1') interatomic distance is 0.03 Å smaller than the experimental value, whereas the corresponding difference in the structure of the cocrystal **C** is ~0.015 Å. The total energy of the cocrystal **C** is 21.68 kcal lower than that of the cocrystal **B**, which means that the cocrystal **B** is thermodynamically less stable.

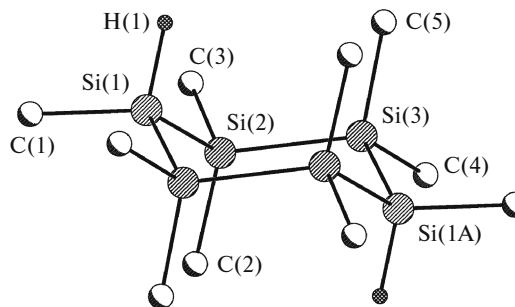


Fig. 3. Overall view of molecule **5b**. The hydrogen atoms, except for H(1), are omitted.

The X-ray diffraction pattern of the crystals of dihydrocyclosilane **4** shows that the structure of **4** is insufficiently ordered for single-crystal X-ray diffraction study. The molecular and crystal structure of dihydrocyclosilane **5b** was determined. Molecule **5b** occupies a special position on an inversion center (Fig. 3). The six-membered ring adopts a chair conformation with the Si(1) atom and the symmetrically equivalent Si atom deviating from the basal plane by 1.04 Å. The hydrogen atoms are in pseudoaxial positions. The Si—Si bonds are somewhat shorter than those in compounds **7** and **8**, the variations in the Si—Si and Si—C bond lengths being within experimental error. In the crystal of **5b**, all intermolecular contacts correspond to usual van der Waals interactions.

Thermotropic phase behavior of cyclosilanes 1–4, 5b, and 6. Unfortunately, attempts to isolate cyclosilane **7** in individual form failed. We studied thermotropic phase transitions of cyclosilanes **1–4**, **5b**, and **6** by differential scanning calorimetry (DSC), polarization microscopy, and X-ray diffraction. Thermal stability of these compounds was studied by thermogravimetric analysis (TGA) (Table 2).

Thermogravimetric analysis showed that most of the compounds under study are characterized by a very low sublimation temperature (see Table 2). Thus, the weight loss started almost immediately once crystals began to melt. Hence, in some cases DSC was not used to determine the isotropization temperature T_i . The temperature range of isotropization was determined by X-ray diffraction and polarization microscopy (see Table 2). It should be noted that the cyclosilanes under consideration are characterized also by sensitivity to X-ray radiation. Taking into account this fact, we chose special conditions for X-ray data collection. Each sample was subjected to X-ray radiation for no more than 2 h.

X-ray diffraction study showed that all the cyclosilanes, except for cyclosilane **4**, are crystalline compounds at 20 °C. According to the DSC data, cyclosilane **4** does not crystallize even at negative temperatures, *i.e.*, this compound is uncrystallizable. Let us first consider the group of crystallizable cyclosilanes. According to the DSC

Table 2. Temperatures (T) and enthalpies (ΔH) of the phase transitions and the sublimation temperatures (T_s) of cyclosilanes **1**–**4**, **5b**, and **6**

Cyclo- silane	$\Sigma\Delta V_i$ / \AA^3	$T/^\circ\text{C}$ ($\Delta H/\text{J g}^{-1}$)					$T_s/^\circ\text{C}$
		crystal ↓ mesophase	crystal ↓ melt	mesophase ↓ melt	mesophase ↓ crystal	melt ↓ mesophase	
1	387.8	79 (46) ^a		— ^b	60 (47) ^a		120 ^c
		82 ^d	—	200–240 ^d	—		207 ^e
		79–81 ^f		>260 ^f			
2	381.7	93 (47.1) ^a		— ^b	55 (43) ^a		125 ^c
		90 ^d	—	140 ^d	—		218 ^e
		98–102 ^f		160 ^f			
3	381.7	89 (44.9) ^a		132 (1.4) ^a	53 (42) ^a		154 ^c
		90 ^d	—	145 ^d	—		225 ^e
		97–103 ^f		162 ^f			
4	355.5	— ^g	—	70 (2.2) ^a		11 (2.4) ^a	100 ^c
				65 ^d	—	—	201 ^e
5b	355.5	60 (52.1) ^{a,i}	73 (58.4) ^{a,h}	85 (3.9) ^{a,i}	9 (50) ^a	42 (3.9) ^a	143 ^c
		50 ^d	—	72 ^d	—	—	226 ^e
		66–71.5 ^f		87–90 ^f			
6	357.4		146 (92) ^a				152 ^c
		—	155 ^d	—	—		360 ^e
			133–160 ^f				

^a The DSC data.^b Isotropization is shielded by sublimation.^c The temperature at which the weight loss was 2%.^d X-ray diffraction data.^e The temperature at which the weight loss was 70%.^f Polarization microscopy.^g Cyclosilane does not crystallize.^{h,i} Two successive (^hfirst and ⁱsecond) heatings were carried out.

data, these compounds do not undergo solid-phase transitions at negative temperatures, *i.e.*, only one crystal modification is typical of these compounds under usual conditions.

The melting points T_m and melting enthalpies ΔH_m of the crystalline phases of cyclosilanes were determined by DSC. These parameters depend substantially on the nature of functional groups at the Si atom (see Table 2). According to the results of X-ray diffraction study and polarization microscopy, only one of crystallizable cyclosilanes, *viz.*, 1,3-dihydroxycyclosilane **6**, is transformed into an isotropic melt at T_m , the initial crystal structure being restored only partially upon cooling from the melt. It should be noted that T_m and ΔH_m for cyclosilane **6** are much higher than those for other cyclosilanes (see Table 2). This is evidence for the presence of a perfect system of OH bonds in the crystal of cyclosilane **6**, resulting in enhancement of thermal stability of the crystals. The cleavage of the OH-bond system upon the crystal–melt transition makes a substantial contribution to ΔH_m .

Cyclosilanes **1**–**3** and **5b** undergo the reversible crystal–mesophase phase transition at T_m . The transition to

the mesomorphic state is accompanied by a considerable change in the scattering pattern. Thus, changes in the angular positions of reflections and a substantial decrease in the number of reflections are observed (Fig. 4, *b* and 5, *b*). A sharp decrease in the intensity of reflections with increasing scattering angle and the appearance of considerable diffuse scattering, which are observed in the X-ray diffraction patterns measured at temperatures higher than T_m , are also typical of mesomorphic structures. According to the DSC data, the mesophase is substantially overcooled and the enthalpies of the mesophase–crystal transitions of the mesomorphic crystallizable cyclosilanes are given in Table 2.

According to the DSC data, cyclosilane **5b** undergoes crystal–mesophase–isotropic melt transitions at temperatures lower than the onset of sublimation (see Table 2 and Fig. 6). The above-mentioned structural transitions cannot be distinguished in the first heating scan under the experimental conditions, and the DSC curve has only one broad endothermic peak in the temperature range of 25–91 °C (see Fig. 6, curve *I*). Two endothermic peaks corresponding to the crystal–mesophase and mesophase–isotropic melt transitions (see Table 2)

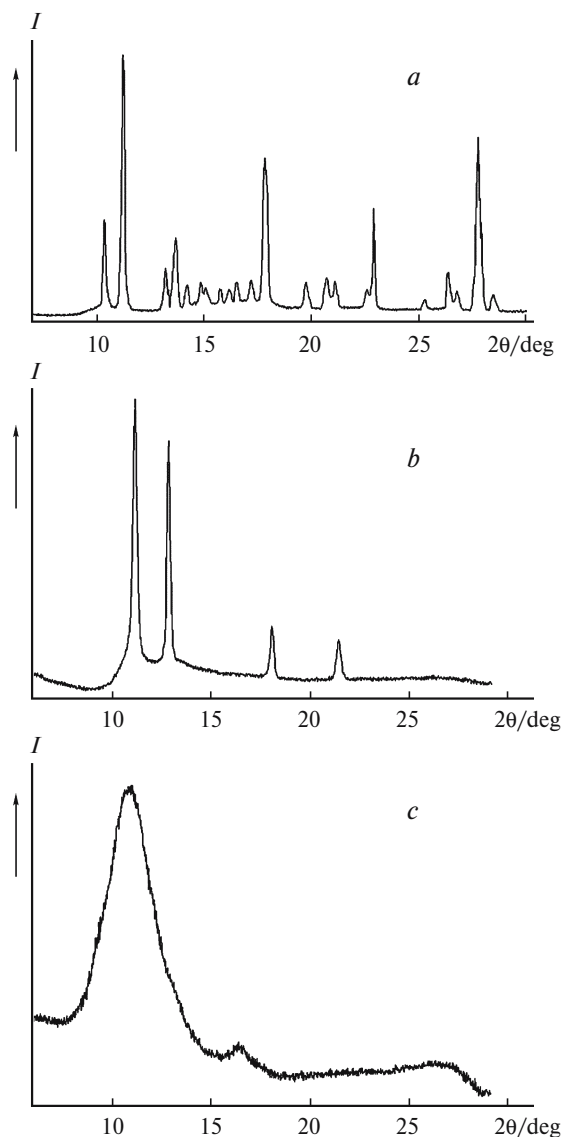


Fig. 4. X-ray diffraction patterns of cyclosilane **3** at 20 (a), 90 (b), and 145 °C (c).

are observed in the repeated heating scan (see Fig. 6, curve 3).

The transformation of cyclosilanes **1–3** and **5b** from the crystalline to mesomorphic state was confirmed by polarization microscopy (Fig. 7, see Table 2), which also revealed a mesomorphic structure for uncrystallizable silane **4**. Study by polarization microscopy showed that the mesophase of cyclosilanes is optically isotropic when viewed through crossed polaroids. However, a cellular texture typical of plastic crystals is observed for this mesophase without crossed polaroids.

The plastic-crystalline behavior and cubic symmetry of the mesophase were confirmed by X-ray diffraction. The X-ray diffraction patterns of the mesophases of cyclosilanes **1–3** have only four reflections. For these

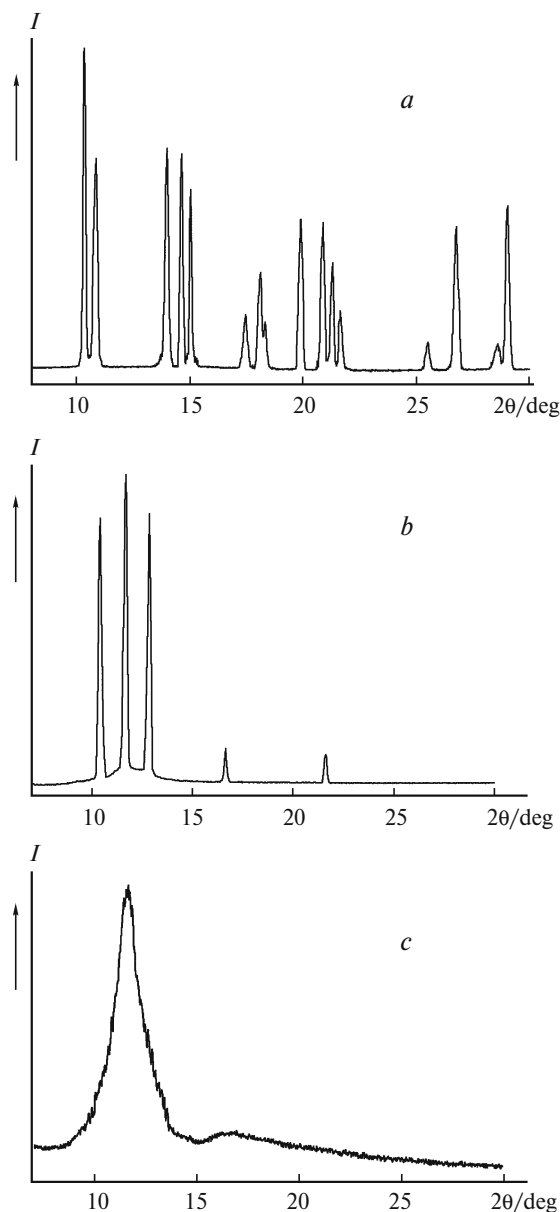


Fig. 5. X-ray diffraction patterns of cyclosilane **5b** at 20 (a), 50 (b), and 72 °C (c).

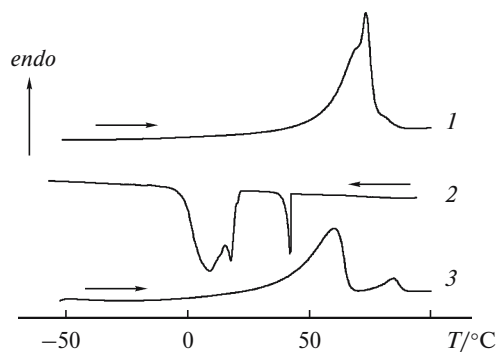


Fig. 6. DSC curves for cyclosilane **5b** in the first heating (1), cooling (2), and second heating (3) scans.

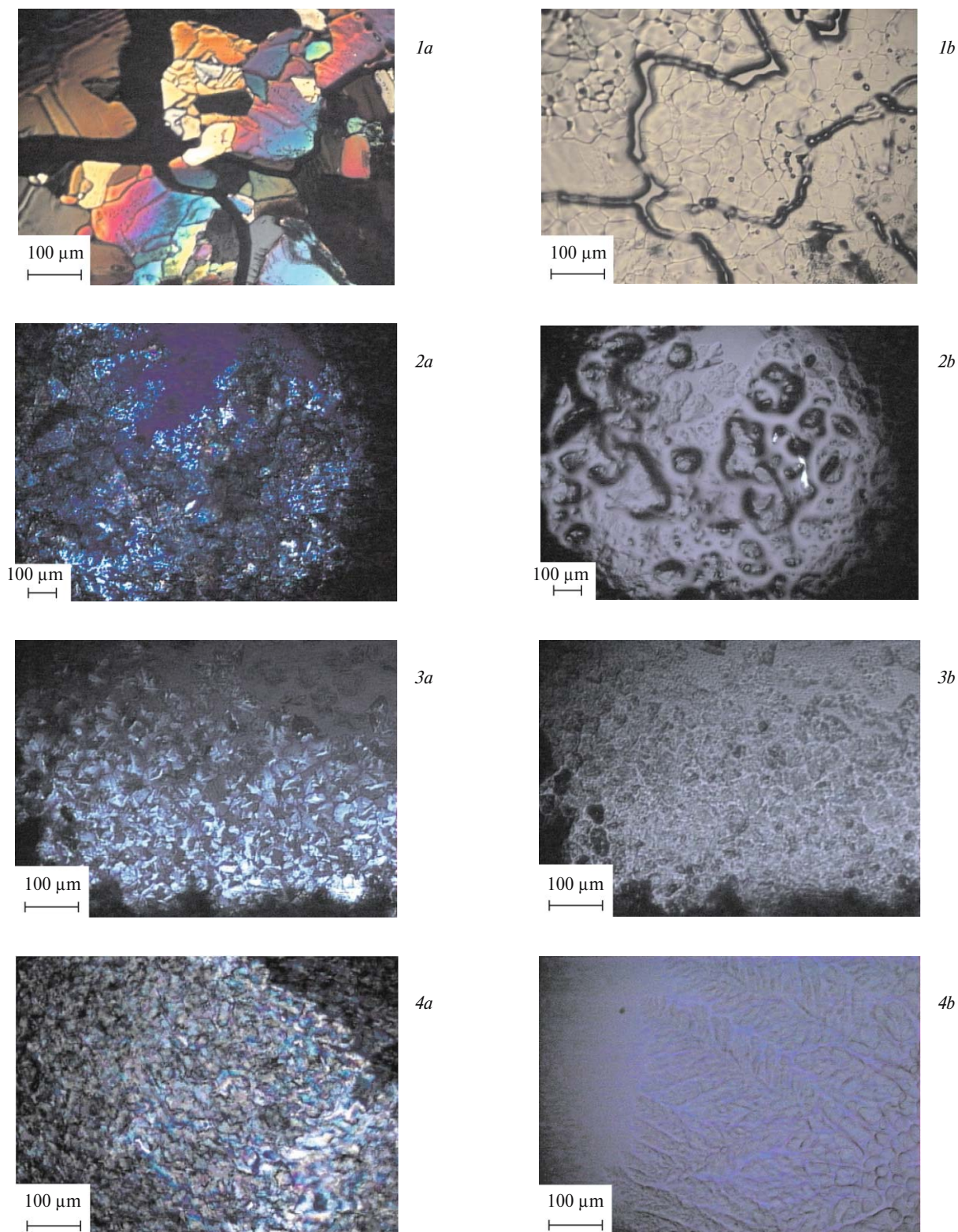


Fig. 7. Optical textures of cyclosilanes **1** (*1*), **3** (*2*), **4** (*3*), and **5b** (*4*): *a*, at 20 °C in the crystalline state (crossed polaroids); *b*, in the plastic-crystalline state (polaroids are not crossed, usual light).

* Figure 7 is available in full color in the on-line version of the journal (<http://www.springeronline.com>) and on the web site of the journal (<http://russchembull.ru>).

reflections, the ratio between $\sin^2\theta$ is 3 : 4 : 11 : 12 (cyclosilanes **1** and **2**) or 3 : 4 : 8 : 11 (cyclosilane **3**, see Fig. 3, *b*), which is indicative of the formation of a face-centered cubic (fcc) unit cell in the mesophase ($Z = 4$). For the fcc unit cells of cyclosilanes **1–3**, the parameter a at 90 °C is 13.94, 13.74, and 13.73 Å, respectively. At the same temperature, the parameter a for the fcc unit cells of cyclosilanes **2** and **3** is slightly smaller than that of the starting cyclosilane **1**, which is quite consistent with the van der Waals volumes of the molecules $\Sigma\Delta V_i$ (see Table 2). It should be noted that the packing of globular molecules in a fcc unit cell is the closest one. The reflections in the X-ray diffraction patterns of cyclosilanes **1** and **2** are indexed as 111, 200, 311, and 222 reflections, and the reflections in the X-ray diffraction pattern of cyclosilane **3** are indexed as 111, 200, 220, and 311 reflections for the fcc unit cells.

The X-ray diffraction pattern of the mesophase of cyclosilane **5b** is somewhat different (see Fig. 5, *b*). This pattern contains five reflections with the $\sin^2\theta$ ratio of 4 : 5 : 6 : 10 : 17, which is also characteristic of cubic systems but with other than fcc unit cells. In the study by polarization microscopy, the mesophase of cyclosilane **5b** was found to be optically isotropic and, consequently, the cubic symmetry of this mesophase was confirmed. Unfortunately, the small number of observed reflections and characteristic features of X-ray diffraction patterns of plastic crystals did not allow us to reveal systematic absences and determine the space group. However, simple calculations enable one to estimate the number of molecules Z per cubic unit cell of cyclosilane **5b**. Actually, knowing the sums of the van der Waals volumes of the increments $\Sigma\Delta V_i$ (see Table 2) for the atoms involved in cyclosilane molecules, the packing coefficient k of the molecules in the mesophase can be calculated by the equation $k = X \cdot \Sigma\Delta V_i / V_{\text{cell}}$ (X is the number of atoms per unit cell and V_{cell} is the unit cell volume). For the fcc unit cells ($Z = 4$) of cyclosilanes **1–3**, k are 0.57 (at 80 °C), 0.60 (at 90 °C), and 0.60 (at 92 °C), respectively. These values agree well with the published data for plastic crystals.¹³ The satisfactory packing coefficient $k = 0.60$ for the cubic unit cell of cyclosilane **5b** was obtained only on the assumption that $Z = 8$. The reflections were indexed as 200, 210, 211, 310, and 410 reflections, and the unit cell parameter a at 50 °C is 16.91 Å.

We are coming now to uncrystallizable cyclosilane **4**. Only one endothermic effect characterized by a very low enthalpy was observed at 70 °C in the DSC curves measured for cyclosilane **4** on heating (see Table 2). A glass transition step at the glass transition temperature (T_g) of -110 – -120 °C is pronounced in the DSC curves both on heating and cooling. At 10 °C, cyclosilane **4** is a wax-like nontransparent substance, which is easily subjected to deformation. This fact, along with the DSC data, sug-

gests that cyclosilane **4** exists in the mesomorphic state at temperatures lower $T_i = 70$ °C and is transformed into mesomorphic glass at temperatures lower T_g . This assumption is confirmed by the results of X-ray diffraction study. The X-ray diffraction patterns of cyclosilane **4** measured at temperatures lower T_i are typical of mesomorphic structures and are similar to the X-ray pattern of the mesophase of cyclosilane **5b** (see Fig. 5, *b*). However, only three reflections were observed for cyclosilane **4**, and the ratio between $\sin^2\theta$ for these reflections was 4 : 5 : 16, which suggests that the mesophase has cubic symmetry. The similarity between the chemical structures of cyclosilanes **4** and **5b** and the identity of the angular positions for two reflections observed for their mesomorphic state suggest the identity of their packings in the cubic unit cell. By contrast, the observed reflections for cyclosilane **4** can be indexed as 200, 210, and 400 reflections, and the calculated unit cell parameter a is 16.67 Å at 10 °C, which is quite consistent with the unit cell parameter of cyclosilane **5b** calculated for higher temperatures.

According to the results of polarization microscopy and X-ray diffraction analysis, isotropization of cyclosilanes **1–4** and **5b** occurs in a wide temperature range (see Table 2). Typical X-ray diffraction patterns of melts of cyclosilanes are shown in Figs 4, *c* and 5, *c*. Thus, the X-ray diffraction pattern of cyclosilane **5b** measured at 72 °C contains only one amorphous halo with a maximum at $2\theta = 11.5^\circ$ (see Fig. 5, *c*).

To summarize, investigation of thermotropic phase transitions of a series of bifunctional cyclosilanes showed that most of these compounds can be transformed into a plastic-crystalline mesophase. An exception is dihydroxycyclosilane **6**. All data for the starting cyclohexasilane **1** are in complete agreement with the published data.^{9,10} The replacement of two methyl groups in cyclohexasilane **1** with the Cl or H atoms leads to a substantial decrease in the temperature range of existence of the mesophase primarily due to a decrease in its high-temperature boundary. The crystal–mesophase and mesophase–melt transition temperatures depend substantially on the nature of the substituents but are virtually independent of their spatial arrangement. One of mesomorphic silanes, *viz.*, uncrystallizable 1,3-dihydrocyclosilane **4**, exists in the plastic-crystalline state throughout the temperature range below T_i , and is transformed into a plastic-crystalline glass below T_g .

Experimental

The ²⁹Si NMR spectra were recorded on a Bruker WP-400 SY spectrometer (79.46 MHz) with Me₄Si as the internal standard. The IR spectrum was measured in the region of 400–3700 cm^{−1} on a Specord M-82 spectrophotometer in a thin layer between KBr windows. The temperatures and enthalpies of phase transi-

tions of cyclosilanes **1**–**4**, **5b**, **6**, and **7** were determined by DSC on a Mettler-Toledo-822e calorimeter according to a standard procedure, the heating and cooling rate was 10 K min⁻¹, and the sample weight was ~6 mg. The sublimation temperatures were determined in argon by TGA on a Derivatograph-C instrument (MOM, Hungary), the heating rate was 5 K min⁻¹, and the sample weight was ~20 mg. X-ray diffraction studies were carried out in the transmission mode on a DRON-3M diffractometer (Cu-K α radiation, Ni filter) equipped with a high-temperature chamber; the temperature was maintained within ± 1 °C. The phase state of the samples was determined by optical polarization microscopy using an Axiolab Pol microscope (Zeiss) equipped with a Linkam computer-controlled hot-stage.

Cyclohexasilane **1** was prepared in 75% yield according to a known procedure.¹⁴ Diethyl ether was dried by refluxing followed by distillation under a stream of argon over sodium metal in the presence of benzophenone. Carbon tetrachloride and petroleum ether were dried by distillation under a stream of argon over P₂O₅. Heptane and acetyl chloride were distilled under a stream of argon immediately before use, Et₃N was distilled under a stream of argon over NaOH granules, and SbCl₅ (Merk) and LiAlH₄ (Aldrich) were used without additional purification. All reactions were carried out under dry argon.

1,3-Dichlorodecamethylcyclohexasilane (2) and 1,4-dichlorodecamethylcyclohexasilane (3). A solution of SbCl₅ (72.5 g, 0.242 mol) in anhydrous CCl₄ (200 mL) was added dropwise with vigorous stirring to a solution of cyclohexasilane **1** (60 g, 0.172 mol) in anhydrous CCl₄ (350 mL) at 0–5 °C. The reaction mixture was stirred at 0–5 °C for 1 h and at 20 °C for 12 h. The precipitate of Me₂SbCl₃ was filtered off and washed with petroleum ether (3 \times 20 mL). The solvents were removed from the filtrate *in vacuo*. The residue was extracted with petroleum ether (5 \times 20 mL) and the solvent was removed. A mixture of structural isomers **2** and **3** (~1 : 1) was obtained in a yield of 45.2 g (67.4%).

1,3-Dihydrodecamethylcyclohexasilane (4) and 1,4-dihydrodecamethylcyclohexasilane (5). A suspension of LiAlH₄ (11.3 g, 0.082 mol) in anhydrous diethyl ether (40 mL) was slowly added dropwise to an isomeric mixture of dichlorocyclosilanes **2** and **3** (15.5 g, 0.04 mol) in anhydrous diethyl ether (150 mL) at 0–5 °C. The reaction mixture was warmed to room temperature and stirred for 6 h. Then a mixture of ice (50 g) and concentrated HCl (5 mL) was slowly added to the reaction mixture. The organic layer was separated, and the aqueous layer was extracted with petroleum ether (3 \times 5 mL). The combined organic phases were dried with Na₂SO₄. The solvents were removed at room temperature *in vacuo*. Anhydrous diethyl ether (1 mL) was added to the residue (11.3 g, 88.6%) containing cyclosilanes **4** and **5**, and the mixture was cooled to –20 °C. The crystals that precipitated (2.75 g, 43.1% of the amount of the starting cyclosilane **3**) were filtered off and recrystallized from anhydrous diethyl ether (0.5 mL). *trans*-1,4-Dihydrocyclohexasilane **5b** was obtained in a yield of 1.3 g, m.p. 63–64 °C. ²⁹Si NMR (C₆D₆), δ : –40.91 (SiMe₂); –68.63 (SiMeH). IR, ν /cm⁻¹: 2070 (Si–H).

1,3-Dihydroxydecamethylcyclohexasilane (6), 1,4-dihydroxydecamethylcyclohexasilane (7) and decamethyl-7-oxahexasilnorbornane (8). A solution of a mixture dichlorocyclosilanes **2** and **3** (22.0 g, 0.0567 mol) in anhydrous diethyl ether (100 mL) and a solution of Et₃N (30.0 g, 0.297 mol) in petroleum ether (100 mL) were added dropwise with vigorous stirring simultaneously from two dropping funnels to a mixture of petroleum

ether (100 mL) and deaerated water (75 mL) for 1.5 h. The reaction mixture was stirred until both phases were clarified (~1 h). The organic layer was separated, and the solvent and excess Et₃N were removed *in vacuo*. The residue (20.1 g) was suspended in petroleum ether (15 mL). The crystals that formed were filtered off and washed with petroleum ether. 1,3-Dihydroxycyclohexasilane **6** was obtained in a yield of 4.5 g (45.1% of the amount of the starting cyclosilane **2**). After recrystallization from heptane, cyclosilane **6** was obtained in a yield of 4.2 g, m.p. 124–126 °C. ²⁹Si NMR (acetone-d₆), δ : 15.81 (SiOH); –38.92 (Me₂SiSiSiMe₂); –40.17 (HOSiSiSiMe₂); –40.82 (HOSiSiSiOH). IR, ν /cm⁻¹: 3325 (OH). MS, m/z (I_{rel} (%)): 334 [M – H₂O]⁺ (11.9), 319 [M – H₂O – Me]⁺ (4.2), 293 (13.0), 259 (18.5), 245 (12.8), 217 (13.5), 189 (13.0), 175 (18.1), 147 (14.4), 117 (40.6), 73 [SiMe₃]⁺ (100).

After separation of cyclosilane **6**, the mother liquor was concentrated, and the crystals that precipitated were filtered off and recrystallized from diethyl ether. A mixture of 1,4-dihydroxycyclohexasilane **7** and bridged compound **8** (in a ratio of 1 : 2) was obtained in a yield of 3.5 g. ²⁹Si NMR (acetone-d₆), δ : **7** – 15.01 (SiOH); –40.04 (SiMe₂); **8** – 14.48 (MeSiO); –35.48 (SiMe₂).

1,3-Dichlorodecamethylcyclohexasilane (2). 1,3-Dihydroxycyclohexasilane **6** (4.2 g, 11.9 mmol) was suspended in cold acetyl chloride (15 mL). The reaction mixture was stirred at 20 °C for 10 h. After removal of excess acetyl chloride and acetic acid that formed during the reaction, a mixture of *cis* and *trans* isomers of 1,3-dichlorocyclohexasilane **2** was obtained in a yield of 4.6 g (99.1%). ²⁹Si NMR (CDCl₃), δ : 16.48, 15.95 (SiCl); –36.89, –37.35 (Me₂SiSiSiMe₂); –38.75, –39.12 (ClSiSiSiMe₂); –42.34, –44.35 (ClSiSiSiCl).

1,4-Dichlorodecamethylcyclohexasilane (3). A mixture of compounds **7** and **8** (3.5 g) was dissolved in acetyl chloride (15 mL) and then water (1.5 mL) was added dropwise at 0–5 °C. The reaction mixture was stirred at 20 °C for 12 h. Excess acetyl chloride and acetic acid that formed during the reaction were removed *in vacuo*, and a mixture of *cis* and *trans* isomers of 1,4-dichlorocyclohexasilane **3** was obtained in a yield of 3.7 g (95.1%). ²⁹Si NMR (CDCl₃), δ : 16.81, 16.34 (SiCl); –39.41, –39.69 (SiMe₂).

1,3-Dihydrodecamethylcyclohexasilane (4). A suspension of LiAlH₄ (0.4 g, 10.8 mmol) in anhydrous diethyl ether (10 mL) was added dropwise to a solution of 1,3-dichlorocyclohexasilane **2** (2.1 g, 5.4 mmol) in anhydrous diethyl ether (15 mL). The reaction mixture was stirred at 20 °C for 3 h. Then ice (10 g) and concentrated HCl (2 mL) were added to the reaction mixture. The ethereal layer was separated, and the aqueous layer was extracted with petroleum ether (3 \times 5 mL). The combined organic phases were dried with Na₂SO₄. The solvents were removed at room temperature *in vacuo*, and 1,3-dihydrocyclohexasilane **4** was obtained as a wax-like substance in a yield of 1.6 g (92.6%). ²⁹Si NMR (CDCl₃), δ : (*cis* and *trans* isomers): –40.42, –40.80 (Me₂SiSiSiMe₂); –40.90, –41.17 (HSiSiSiMe₂); –41.39, –41.53 (HSiSiSiH); –67.11, –67.95 (SiH). IR, ν /cm⁻¹: 2070 (Si–H).

1,4-Dihydrodecamethylcyclohexasilane (5). A mixture of *cis* and *trans* isomers of 1,4-dihydrocyclohexasilane **5** was prepared in a yield of 1.5 g (91.2%) from 1,4-dichlorocyclohexasilane **3** (2.0 g, 5.15 mmol) and LiAlH₄ (0.4 g, 10.8 mmol) analogously to the synthesis of cyclosilane **4**. Anhydrous diethyl ether (1 mL) was added to the reaction mixture, and the mixture

Table 3. Principal characteristics of X-ray diffraction study and crystallographic data for **B**, **C**, **5b**, and **8**

Parameter	B	C	5b	D
Molecular formula	C ₁₅ H ₄₆ O ₂ Si ₉	C ₁₅ H ₄₆ O ₂ Si ₉	C ₁₀ H ₃₂ Si ₆	C ₁₀ H ₃₀ OSi ₆
Molecular weight	510.34	365.29	320.90	334.8
<i>T</i> /K	110(2)	110(2)	127(2)	110(2)
<i>a</i> /Å	10.289(2)	9.2421(16)	6.6458(14)	9.788(1)
<i>b</i> /Å	10.387(3)	11.693(2)	9.437(2)	13.020(2)
<i>c</i> /Å	15.518(4)	16.170(3)	9.923(2)	16.014(2)
α /deg	102.224(6)	99.116(4)	116.476(4)	90
β /deg	97.585(6)	99.746(4)	101.882(5)	100.139(3)
γ /deg	97.120(6)	109.697(4)	97.894(4)	90
<i>V</i> /Å ³	1586.7(7)	1577.2(5)	526.1(2)	2008.8(4)
<i>d</i> _{calc} /g cm ⁻³	1.068	1.077	1.013	1.107
Space group	<i>P</i> $\bar{1}$	<i>P</i> $\bar{1}$	<i>P</i> $\bar{1}$	<i>P</i> 2(1)/ <i>c</i>
<i>Z</i>	2	2	1	4
2 θ _{max} /deg	56	60	60	56
<i>F</i> (000)	556	556	176	728
Scanning mode	Ω	ω	Ω	ω
Number of measured reflections	11634	13146	4914	11803
Number of independent reflections	7623	9050	2999	4835
<i>R</i> _{int}	0.0256	0.0252	0.0349	0.0415
Number of observed reflections with <i>I</i> > 2 σ (<i>I</i>)	5192	5808	2067	2863
Number of parameters in refinement	250	252	137	274
Absorption coefficient/cm ⁻¹	3.84	3.88	3.79	4.03
<i>R</i> ₁ (<i>I</i> > 2 σ (<i>I</i>))	0.0593	0.0459	0.0669	0.0572
<i>wR</i> ₂	0.1329	0.1294	0.1634	0.1220

was cooled to -20 °C. The crystals that formed (0.7 g) were filtered off and recrystallized from diethyl ether (0.5 mL). *trans*-1,4-Dihydrocyclohexasilane **5b** was obtained in a yield of 0.6 g. ²⁹Si NMR (CDCl₃), δ : -40.79 (SiMe₂); -68.55 (SiH). IR, ν /cm⁻¹: 2090 (Si—H).

After separation of *trans*-1,4-dihydrocyclohexasilane **5b**, diethyl ether was removed from the residue, and *cis*-1,4-dihydrocyclohexasilane **5a** was obtained in a yield of 0.7 g. ²⁹Si NMR (CDCl₃), δ : -40.52 (SiMe₂); -67.57 (SiH). IR, ν /cm⁻¹: 2085 (Si—H).

X-ray diffraction study of crystals B, C, D, and 5b. Crystallographic parameters and principal characteristics of X-ray diffraction study are given in Table 3. X-ray diffraction data sets were collected on a Bruker Smart CCD 1000 diffractometer. The structures were solved by direct methods and refined by the full-matrix least-squares method against *F*² with anisotropic displacement parameters for nonhydrogen atoms. The hydrogen atoms of the hydroxy groups were localized from difference Fourier syntheses and refined isotropically. All calculations were carried out using the SHELXTL PLUS (version 5.10) program package.¹⁵

In the crystals of dichlorododecamethylsilanes, a static disorder of the chlorine atoms, which occurs due to superposition of molecules **2** and **3**, was revealed. The unit cell parameters are *a* = 17.811(4) Å, *b* = 9.956(2) Å, *c* = 13.738(3) Å, β = 109.18(2)°, space group *C*2/*c*.

Quantum-chemical calculations. All calculations were carried out with full geometry optimization, the PBE exchange-correlation functional, and the basis set of plane waves (kinetic energy cutoff was 25 Ry) using the CPMD program.¹⁶ The

ultrasoft pseudopotentials¹⁷ were utilized to account for the core electrons. Calculations for the crystals **B** and **C** were carried out under periodic boundary conditions with consideration for only Γ points in the Brillouin zone using the experimental unit cell parameters. Isolated molecules **7** and **8** were modelled with a unit cell of dimensions 15×15×15 Å.

This study was financially supported by the Russian Foundation for Basic Research (Project Nos 03-03-32214 and 02-07-90165).

References

1. K. Kumar and M. H. Litt, *J. Polym. Sci., Polym. Lett.*, 1988, **26**, 25.
2. A. Kleewin and H. Stüger, *Monatsh. Chem.*, 1999, **130**, 69.
3. D. Yu. Larkin, N. A. Chernyavskaya, and A. I. Chernyavskii, *Tez. dokl., VIII Mezhdunar. konf. po khimii i fizikokhimii oligomerov "Oligomery-2002"* [Abstr. of Papers, VIII Int. Conf. on Chemistry and Physical Chemistry of Oligomers "Oligomers-2002"] (Moscow—Chernogolovka, September 9—14, 2002), Moscow—Chernogolovka, 2002, 75 (in Russian); A. I. Chernyavskii, D. Yu. Larkin, and N. A. Chernyavskaya, *Izv. Akad. Nauk, Ser. Khim.*, 2002, 165 [*Russ. Chem. Bull., Int. Ed.*, 2002, **51**, 175]; D. Yu. Larkin, N. A. Chernyavskaya, and A. I. Chernyavskii, *Book of Abstr. Int. Symp. "Modern Trends in Organometallic and Catalytic Chemistry"* (Moscow, Russia, May 18—23, 2003), Moscow, 2003, 199; D. Yu. Larkin, N. A. Chernyavskaya, and A. I. Chernyavskii, *Tez.*

- dokl., III Vseros. Karginskoi konf. "Polimery-2004" [Abstrs. of Papers, III All-Russian Kargin Conf. "Polymers-2004"], (Moscow, January 27–February 1, 2004), Moscow, 2004, 103 (in Russian); A. I. Chernyavskii, D. Yu. Larkin, M. I. Buzin, E. G. Kononova, and N. A. Chernyavskaya, *Zh. Prikl. Khim.*, 2004, **77**, 289 [*Russ. J. Appl. Chem.*, 2004, **77** (Engl. Trans.)].
4. W. Wojnowski, B. Dreczewski, A. Herman, K. Peters, E. M. Peters, and H. G. von Schnering, *Angew. Chem.*, 1985, **97**, 978.
5. B. Derczewski and W. Wojnowski, *J. Prakt. Chem.*, 1990, **332**, 229.
6. E. Hengge and M. Eibl, *J. Organomet. Chem.*, 1992, **428**, 335.
7. A. Spielberger, P. Gspaltl, H. Siegl, E. Hengge, and K. Gruber, *J. Organomet. Chem.*, 1995, **499**, 241.
8. A. A. Korlyukov, D. Yu. Larkin, N. A. Chernyavskaya, M. Yu. Antipin, and A. I. Chernyavskii, *Mendeleev Commun.*, 2001, 195.
9. D. W. Larsen, B. A. Soltz, F. E. Sary, and R. West, *Chem. Commun.*, 1978, 1093.
10. D. W. Larsen, B. A. Soltz, F. E. Sary, and R. West, *J. Phys. Chem.*, 1980, **84**, 1340.
11. M. Möller, D. Oelfin, and B. Wunderloich, *Mol. Cryst. Liq. Cryst.*, 1989, **173**, 101.
12. A. A. Korlyukov, N. A. Chernyavskaya, M. Yu. Antipin, K. A. Lyssenko, and A. I. Chernyavskii, *Khim. Geterotsikl. Soedin.*, 2005, 624 [*Chem. Heterocycl. Compd.*, 2005, **41**, 536 (Engl. Transl.)].
13. W. J. Dunning, in *The Plastically Crystalline State. (Orientationally-Disordered Crystals)*, Ed. N. Sherwood, Wiley, New York—London, 1979, 1.
14. A. I. Chernyavskii and B. G. Zavin, *Izv. Akad. Nauk, Ser. Khim.*, 1997, 1513 [*Russ. Chem. Bull.*, 1997, **46**, 1449 (Engl. Transl.)].
15. G. M. Sheldrick, *SHELXTL97, Version 5.10*, Bruker AXS Inc., Madison (WI-53719, USA), 1997.
16. J. Hutter, P. Ballone, M. Bernasconi, P. Focher, E. Fois, S. Goedecker, M. Parrinello, and M. Tuckerman, *CPMD*, v. 3.7.2, MPI für Festkörperforschung and IBM Zurich Research Laboratory, Zurich, 1995–2001.
17. D. Vanderbilt, *Phys. Rev.*, 1985, **B41**, 7892.

Received October 20, 2004;
in revised form February 22, 2005